Dynamics of a dissolution front for solids under stress

Chaouqi Misbah

Groupe de Recherche sur les Phénomènes Hors de l'Equilibre, Laboratoire de Statistique et Probabilités, Université Joseph Fourier (CNRS), Grenoble, France

François Renard[1] and Jean-Pierre Gratier

Laboratoire de Géophysique Interne et Tectonophysique-Centre National de la Recherche Scientifique, Université Joseph Fourier, Grenoble, France

Klaus Kassner

Institut für Theoretische Physik, Otto-von-Guericke-Universität Magdeburg, Magdeburg, Germany

Received 22 November 2003; revised 3 February 2004; accepted 1 March 2004; published 26 March 2004.

[1] A kinetic study including dissolution process and diffusion of the dissolved molecules for a stressed solid in contact with its solution is analyzed. We estimate a condition fixing the prevailing dissipation mechanism and analyze it with a linear stability criterion. This criterion depends on which process is limiting the rate of dissipation: dissolution at the solid-liquid interface or diffusion in the fluid. For definiteness we focus on recent experiments on various salts, which have shown that grooves, oriented perpendicular to the main compressive stress, develop on the free surfaces of crystals. We provide the characteristic length scale and the time scale for the development of this stress-induced roughening of solid surfaces, which are consistent with the experiments. Finally, we estimate these parameters for relevant geological conditions. *INDEX TERMS:* 3902 Mineral Physics: Creep and deformation; 3939 Mineral Physics: Physical thermodynamics; 3909 Mineral Physics: Elasticity and anelasticity; 5112 Physical Properties of Rocks: Microstructure. **Citation:** Misbah, C., F. Renard, J.-P. Gratier, and K. Kassner (2004), Dynamics of a dissolution front for solids under stress, *Geophys. Res. Lett.*, *31*, L06618, doi:10.1029/2003GL019136.

1. Introduction

[2] The morphological instability [*Asaro and Tiller*, 1972; *Grinfeld*, 1986; *Srolovitz*, 1989] of a free surface of a solid, which is nonhydrostatically stressed, is a very general problem, which is encountered in various circumstances in physics and geophysics. There are several situations (see below) where the instability is limited both by the growth/dissolution process, and by mass diffusion in the liquid bulk phase. This is encountered in many geomaterials where the present instability has been the focus of recent studies with the aim of elucidating the stress-driven morphological instability [*Gal et al.*, 1998; *den Brok and Morel*, 2001].

[3] In experiments on various salt crystals, it has been shown that the free surfaces of crystals under uniaxial stress can develop morphological instabilities [*den Brok and Morel*, 2001; *den Brok et al.*, 2002; *Koehn et al.*, 2004]. The surface of a crystal in contact with its solution does not remain flat when the crystal is pressed and tends to roughen and develop parallel grooves with time. The instability is driven by a competition between mechanical forces on the surface and capillary effects. Extrapolated to crustal conditions, the experiments show that elastic strain energy does play an important role as such energy can modify the minimization of the free energy of a fluid-rock system and drive dissolution-precipitation processes to dissipate stress heterogeneities at the grain scale. Moreover, the grooves may evolve into cracks [*Yang and Srolovitz*, 1993; *Kassner and Misbah*, 1994] and modify strongly the mechanical properties of the rocks.

[4] Here we present a linear stability analysis and apply it to natural examples with conditions corresponding to rocks in the Earth's crust. We provide the characteristic wavelength and the characteristic growth time of the instability. We find that both dissolution and diffusion in the liquid play an essential role.

2. Thermodynamic and Kinetic Analysis

[5] Let us focus on the situation where a semi-infinite solid phase is uniaxially stressed [*den Brok and Morel*, 2001] in contact with its saturated solution (Figure 1). The driving force for the dissolution is the stress, and we first specify how the chemical potential evolves with the stress. We imagine that a mass Δm of the solute is transformed into the solid phase (or vice versa), and compute the Gibbs free energy, ΔG, involved in that transformation. The chemical potential is defined per unit volume, $\Delta\mu = \Delta G/\Delta V$.

$$\Delta G = \Delta F + \Delta(p_f V) \tag{1}$$

where V is the volume and p_f the solute pressure. ΔF is the Helmholz free energy change. If only mechanical work is considered, ΔF is obtained upon integration of the infinitesimal work involved in this transformation.

$$dF = \sigma_{ij} du_{ij} \delta V \tag{2}$$

[1] Also at Physics of Geological Processes, University of Oslo, Oslo, Norway.

0094-8276/04/2003GL019136$05.00

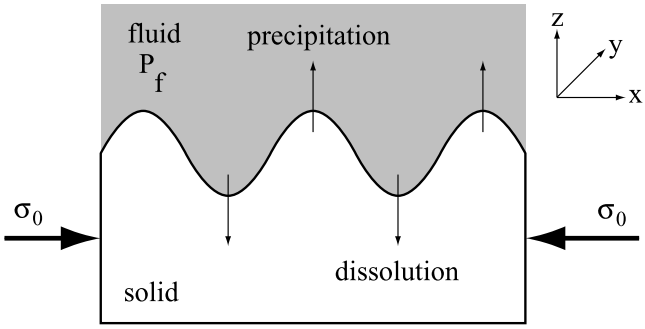

Figure 1. Stress-enhanced morphological instabilities can form on the surface of a solid under stress σ_0, in contact with its solution at a fluid pressure P_f.

where σ_{ij} is the stress tensor and u_{ij} the deformation tensor. Thus

$$dG = \sigma_{ij} du_{ij} \delta V + p_f d(\delta V). \tag{3}$$

For plain strain, [*Cantat et al.*, 1998] show, upon using Hooke's law and integration over a finite transformation ΔV, that $\Delta G = \Delta\mu \Delta V$, where

$$\Delta\mu = \left(1 - \nu^2\right)(\sigma_{nn} - \sigma_{tt})^2/2E + \gamma\kappa \tag{4}$$

is the chemical potential ($\mu_s - \mu_l$), the difference between the chemical potential of a molecule in the solid and that in the solution, referred to unit volume. ν is the Poisson ratio, E [Pa] is the Young modulus, γ [$Pa \cdot m$] is the surface tension, κ [m^{-1}] is the surface curvature, $\sigma_{nn} = n_i \sigma_{ij} n_j$, $\sigma_{tt} = t_i \sigma_{ij} t_j$, where n_i and t_i are the ith components of the normal and the tangent unit vectors to the solid surface.

[6] Let Q denote the ionic concentration product of the dissolution reaction into liquid, and K_{eq} is the thermodynamic equilibrium constant in the absence of stress [*Alkattan et al.*, 1997]. Considering the solute to be an ideal solution, and expanding the chemical potential about the stress-free equilibrium concentration we can write $\Delta\mu = -(Q - K_{eq})RT/(K_{eq}\bar{V}_s)$, where R is the universal gas constant, and $\bar{V}_s$ [$m^3 \cdot mole^{-1}$] is the molar volume. The minus sign tells us that if the solid chemical potential is increased ($\Delta\mu > 0$) then a solid dissolution is implied. Using equation (4) together with the above result, we can write

$$\Delta\mu = \frac{1 - \nu^2}{2E}(\sigma_{nn} - \sigma_{tt})^2 + \gamma\kappa - \frac{(Q - K_{eq})RT}{K_{eq}\bar{V}_s}. \tag{5}$$

It is sometimes customary to write $\Delta\mu = -(Q - K^*_{eq})RT/(K_{eq}\bar{V}_s)$, where

$$K^*_{eq} = K_{eq}\left\{1 + \frac{\bar{V}_s}{RT}\left[\frac{1 - \nu^2}{2E}(\sigma_{nn} - \sigma_{tt})^2 + \gamma\kappa\right]\right\}. \tag{6}$$

The dissolution speed, v_n in $m.s^{-1}$ is proportional to the actual difference in chemical potential. We set

$$v_n = k\bar{V}_s(Q - K^*_{eq})/K_{eq} \tag{7}$$

where v_n is the normal front velocity, and k is a dissolution rate constant [$mole \cdot m^{-2} \cdot s^{-1}$]. From equations (6) and (7) we obtain the dissolution speed as a function of the stress and the actual solute concentration

$$\frac{v_n}{\bar{V}_s k} = \frac{Q}{K_{eq}} - 1 - \frac{\bar{V}_s}{RT}\left[\gamma\kappa + \frac{1 - \nu^2}{2E}(\sigma_{nn} - \sigma_{tt})^2\right]. \tag{8}$$

The relationship between the ionic product Q and the concentration depends on the order of the dissolution-precipitation reaction. Usually $Q \sim c^n$ where c (in $mole.m^{-3}$) is the concentration in the fluid and n is the order of the reaction; $n = 1$ for quartz, whereas $n = 2$ for sodium chlorate and sodium chloride, and $n = 4$ for K-alum. We focus on the case $n = 1$; situations with $n \neq 1$ can be dealt with along the same line. Thus we set $Q = c$ and $K_{eq} = c_{eq}$.

[7] Now the stress configuration in the solid phase for a given surface profile must be determined. When the front is deformed (a dissolution-recrystallization wave) the solute concentration is affected; it depends on the actual front profile. Therefore, the concentration field must also be solved for in a consistent manner.

[8] Let us first address the question of the stress. For a uniaxial stress applied along x we expect the front morphology to be invariant along y (Figure 1). For 2D elasticity one can use the Airy function $\chi(x, z)$ and this quantity is known to obey a bi-harmonic equation $\nabla^4\chi = 0$. For an arbitrary solid profile, the problem can be solved numerically. However, if one is interested in the early stage of the instability, a linear stability analysis is sufficient [*Kassner et al.*, 2001]. In the linear regime the front profile $h(x, t)$ can be written as

$$h = \epsilon \cos(qx)e^{\omega t} \tag{9}$$

where ϵ is the amplitude of deformation, assumed to be small enough for a linear theory to make a sense, q (m^{-1}) is the wavenumber of the deformation and ω (s^{-1}) is the growth (or attenuation) rate that we wish to determine. An instability is signaled by a positive ω.

[9] From [*Cantat et al.*, 1998] one finds that the stress contribution entering equation (8) reads

$$(\sigma_{nn} - \sigma_{tt})^2 = -4\sigma_0^2 qh \tag{10}$$

and the surface tension contribution has the form

$$\gamma\kappa = \gamma q^2 h \tag{11}$$

where we have used the fact that for small deformations, the curvature has the form $\kappa = -\partial^2 h/\partial x^2$ (the minus sign ensures that for a concave solid the chemical potential is increased). $\sigma_0 \equiv \sigma^0_{xx} - \sigma^0_{zz}$ is the difference between the horizontal and the vertical stresses in the initial planar configuration. This is the source of the planar front instability.

[10] Now we address the question of the concentration field. The concentration obeys the diffusion equation in the fluid

$$D\nabla^2 c = \partial c/\partial t. \tag{12}$$

Far ahead of the front the concentration is that corresponding to the planar front under stress. The concentration field perturbation due to the interface deformation decays with z sufficiently away from the interface, while along x it follows the interface deformation. That is, we must have $c = f(z)\cos(qx)\, e^{\omega t}$. Plugging this into equation (12) one obtains $f(z) = Ae^{-\beta z}$, $\beta = \sqrt{q^2 + \omega/D}$, and A is an integration factor to be determined below. Note that the solution that increases exponentially with z has been removed. The concentration field takes the form

$$c = Ae^{-\beta z}\cos(qx)e^{\omega t}. \tag{13}$$

Reporting this along with the contributions of stress (equation (10)) and surface tension (equation (11)) into equation (8), one obtains a relationship between A and ϵ

$$\frac{A}{c_{eq}} = \frac{\bar{V}_s}{RT}\left[\gamma q^2 - \frac{2(1-\nu^2)}{E} q\sigma_0^2\right]\epsilon + \frac{\omega}{\bar{V}_s k}\epsilon. \tag{14}$$

Because c is a small perturbation we have evaluated the above equation at $z = 0$ and not at $z = h$ (this is sufficient if one is only interested in the leading contribution which is linear in the deformation ϵ). Note also that for small deformation, $v_n \simeq \partial h/\partial t = \omega\epsilon\cos(qx)e^{\omega t}$. Finally the closure condition follows from mass conservation, stating that the dissolution mass current across the interface is proportional to the normal surface velocity, namely

$$v_n(c_s - c) = D\mathbf{n}.\nabla c \tag{15}$$

where c_s is the concentration in the solid phase. If the concentration is counted as a number per unit volume, we simply have $c_s = 1/\Omega$ where Ω is the molar volume of the solid. Since the volume occupied by a solute molecule is much larger than that in the solid phase, we have $c_s \gg c$. In the linear regime we are interested in, the mass conservation equation reads

$$c_s\partial h/\partial t = D\partial c/\partial z = -\beta AD\cos qx e^{\omega t} \tag{16}$$

where use has been made of relation (13). This provides us with another relation between A and ϵ. Compatibility with equation (14) yields the sought after dispersion relation

$$\omega\left[1 + \frac{\beta D c_{eq}}{k}\right] = \frac{c_{eq} q D\bar{V}_s}{c_s RT}\left[\frac{2(1-\nu^2)\sigma_0^2}{E} q - \gamma q^2\right]. \tag{17}$$

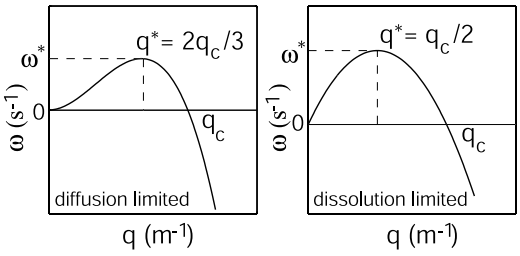

Figure 2. Two shapes of ω (q) (equation (17)) arise depending on which process (dissolution or diffusion) is the slowest. The fastest wavenumber q^* develops with an inverse growth time ω^*. For the diffusion-limited case $\omega \propto q^2 - q^3$, whereas for the dissolution-limited case $\omega \propto q - q^2$.

Table 1. Parameters Used to Calculate the Characteristic Length Scale and Growth Time of the Instability

Parameter	NaCl	NaClO3	K-alum	Quartz	Quartz
T (C)	25	25	25	100	200
D ($m^2 \cdot s^{-1}$)[a]	2E-9	2E-9	2E-9	6.8E-9	1.9E-8
c_{eq} (mole $\cdot$ m^{-3})	5416	9400[c]	300	0.9[d]	4.2[d]
k (mole $\cdot$ $m^{-2} \cdot s^{-1}$)[b]	2.5	2.5	2.5	5E-9[d]	1E-6[d]
$\bar{V}_s$ ($m^3 \cdot mole^{-1}$)	2.7E-5	4.3E-5	14.8E-5	2.3E-5	2.3E-5
E (GPa)	30	49	19	72	72
ν	0.25	0.25	0.25	0.25	0.25
γ (Pa.m)[e]	0.01	0.01	0.01	0.35	0.35

[a] *Applin* [1987].
[b] estimated from *Alkattan et al.* [1997] for NaCl and the same value is used for the other salts.
[c] *Ristic et al.* [1993].
[d] *Rimstidt and Barnes* [1980].
[e] see *Mersmann* [1990] for salts and *Parks* [1984] for quartz.

Since c_s is the concentration of a molar solid mass, we have $c_s\bar{V}_s = 1$. Note that we have set $\beta = \sqrt{q^2 + \omega/D} \simeq q$. This means that ω (the inverse of the time scale for the instability development) is small in comparison to the diffusion of molecules in the solute. More precisely, the diffusion is fast in comparison to the interface evolution time scale. This is the quasi-steady approximation. Depending on which process (diffusion or dissolution) is the slowest one, two limiting forms of the dispersion relation are obtained from equation (17); see Figure 2.

[11] Let us now discuss the implication of our results for the case of salt crystals under stress [*den Brok and Morel*, 2001; *Koehn et al.*, 2004], and other geological systems. The dispersion relationship (17) tells us that $\omega > 0$ for

$$q < q_c \equiv \frac{2\sigma_0^2(1-\nu^2)}{E\gamma}, \quad \lambda_c = \frac{2\pi}{q_c} = \frac{\pi E\gamma}{\sigma_0^2(1-\nu^2)} \tag{18}$$

This is nothing but the thermodynamically optimal wavenumber (or wavelength λ_c) [*Asaro and Tiller*, 1972; *Grinfeld*, 1986; *Srolovitz*, 1989]. Equation (17) informs us, in addition, on the kinetics of the instability as well as on the relative effects of the two competing dissipations, (i) the dissolution process characterized by the kinetic rate constant k, and (ii) the diffusion process signaled by the presence of the diffusion coefficient D. The slowest factor limits the instability development. The instability is limited by diffusion if

$$qDc_{eq}/k \ll 1. \tag{19}$$

In the opposite limit the process would be limited by dissolution. We need to evaluate the wave-number in order to test the above inequality. At the initial stage of the instability it is reasonable to expect this to be given by the fastest growing mode. Let q^* refer to that wavenumber. Let us suppose that the process is limited by dissolution. In that case one obtains from equation (17) that $q^* = q_c/2$. Using the data given by *den Brok and Morel* [2001] for K-alum, we find $\lambda^* = 2\pi/q^* = 51$ μm, which is close to the experimental wavelength of 60 μm. Using Table 1 and the above result we find, on the basis of condition (19), that the dynamics is limited by

Table 2. Comparison Between the Experimental and Theoretical Characteristic Length and Growth Time of the Instability on Different Crystals[a]

Mineral	σ_0 (MPa)	T (C)	λ^*_{diss} (μm)	T^*_{diss}	T^*_{diff}
Experiments					
Sodium chlorate[b]	4	25	150 ± 130	<50h	–
Sodium chlorate[b]	8	25	38 ± 32	<4h	–
K-alum[c]	5	25	60	<25h	–
Theoretical values (Equations (20) and (21))					
Sodium chlorate	4	25	205	100h	**121h**
Sodium chlorate	8	25	51	**6.2h**	1.9h
K-alum	5	25	51	0.5h	**4.9h**
Sodium chloride	8	25	31	**5.9h**	1.9h
Quartz	12	100	1173	**23 Myrs**	1 kyrs
Quartz	25	200	270	**7.8 kyrs**	1.2 yr

[a]The largest time (in bold) between T^*_{diss} and T^*_{diff} characterizes the slowest step that controls the formation of the instability. Application to quartz and NaCl under geological conditions.

[b]*Koehn et al.* [2004].

[c]*den Brok and Morel* [2001], *den Brok et al.* [2002].

diffusion. For sodium chlorate (Table 2), we find for large stresses that the dynamics is limited by dissolution. Upon lowering the stress diffusion becomes competing (stress 8 MPa and 4 MPa in Table 2). At later time coarsening is expected [*Kassner and Misbah*, 1994], so that relation (19) is reinforced due to the decrease of q (coarsening). Thus one expects the diffusion process to override dissolution as the limiting mechanism. For the case of quartz (Table 1), and for the same typical length-scales, one finds that $q^* D c_{eq}/k \gg 1$, so that here dynamics is, beyond any doubt, limited by the dissolution process.

[12] The time scales for the instability evolution are obtained from the dispersion relation. Consider the case where the dynamics is limited by dissolution. The time scale $T^* = 2\pi/\omega^*$ (where $\omega^* = \omega(q^*)$; see Figure 2) for the birth of the instability is given by

$$T^*_{diss} = \frac{2\pi RT}{k\bar{V}_s^2 \gamma q^{*2}} = \frac{2\pi RTE^2\gamma}{k\bar{V}_s^2(1-\nu^2)^2\sigma_0^4}. \qquad (20)$$

Using the theoretical values of q^* and the other parameters (Table 1), one obtains that T^* falls in the typical experimental range within a factor 2 (Table 2). With a similar length-scale, for quartz at 200°C and 25 MPa, (Table 1) one finds that $T^* = 7800$ years. For smaller length-scales (higher stresses) the time scale is lower. For lower temperature, at 100°C, the time scale is found to be of about 23 Myrs.

[13] If the instability is limited by diffusion, from equation (17) one obtains that the fastest growing mode ω^* is obtained for $q^* = 2q_c/3$. The time scale for this mode is given by

$$T^*_{diff} = \frac{4\pi RT}{3\gamma\bar{V}_s^2 D c_{eq} q^{*3}} = \frac{27\pi RTE^3\gamma^2}{16D\bar{V}_s^2 c_{eq}(1-\nu^2)^3\sigma_0^6}. \qquad (21)$$

This situation should occur in [*den Brok and Morel*, 2001] experiments where the characteristic time for diffusion (4.9 h) is greater than for dissolution (0.5 h). If the solution was not stirred, or that the hydrodynamic boundary layer is large in comparison to the ripple wavelength, then diffusion would control ripple formation.

3. Conclusions

[14] The rationale of this study is to use thermodynamic and kinetics derivation to study morphological instabilities on the surface of stressed crystals in contact with a reactive aqueous fluid. The linear stability analysis provides the wavelength and the characteristic growth time of the instability. The characteristic length scales are compatible with recent experimental results on salt crystals [*den Brok and Morel*, 2001; *den Brok et al.*, 2002; *Koehn et al.*, 2004]. An interesting feature is that, depending on systems we encounter, both dissolution and diffusion can act as limiting factors. For sodium chlorate we expect a cross-over from dissolution-limited to diffusion-limited as coarsening proceeds. We find a consistent picture with available experimental data regarding length and time scales, aside from a factor 2 for time.

[15] Under geological conditions, depending on the material, the length-scale of the instabilities is in the range 0.1–1 mm, and the characteristic time scales varies between several hours (sodium chloride), up to several million years (quartz at shallow depth); see Table 2. Applied to various crustal conditions, these results show that this instability should be considered over geological time scales as it modifies the free-energy of a stressed fluid-rock system.

[16] **Acknowledgments.** The project has been supported by the *Centre National de la Recherche Scientifique* (ATI to F. Renard). We would like to thank C. Pequegnat and D. Tisserand for their technical help. We acknowledge J. Schmittbuhl, D. Koehn, D. Dysthe, and D. Clamond for very fruitful discussions, and B. den Brok for the constructive review.

References

Alkattan, M., E. Oelkers, J.-L. Dandurand, and J. Schott (1997), Experimental studies of halite dissolution kinetics. 1. The effect of saturation state and the presence of trace metals, *Chem. Geol.*, *137*, 201–219.

Applin, K. R. (1987), The diffusion of dissolved silica in dilute aqueous solution, *Geochim. Cosmochim. Acta*, *51*, 2147–2151.

Asaro, R., and W. Tiller (1972), Interface morphology development during stress corrosion cracking: Part I, Via diffusion, *Met. Trans.*, *3*, 1789–1796.

Cantat, I., K. Kassner, C. Misbah, and H. Müller-Krumbhaar (1998), Directional solidification under stress, *Phys. Rev. E*, *58*, 6027–6040.

den Brok, S. W. J., and J. Morel (2001), The effect of elastic strain on the microstructure of free surfaces of stressed minerals in contact with an aqueous solution, *Geophys. Res. Lett.*, *28*, 603–606.

den Brok, S. W. J., J. Morel, and M. Zahid (2002), In situ experimental study of roughness development at a stressed solid/fluid interface, in *Deformation Mechanisms, Rheology, and Tectonics: Current Status*, *Geol. Soc. London Spec.*, *200*, 73–83.

Gal, D., A. Nur, and E. Aharonov (1998), Stability analysis of a pressure-solution surface, *Geophys. Res. Lett.*, *25*, 1237–1240.

Grinfeld, M. (1986), Instability of the separation boundary between a non-hydrostatically stressed solid and a melt, *Sov. Phys. Dokl.*, *31*, 831–835.

Kassner, K., and C. Misbah (1994), Nonlinear evolution of a uniaxially stressed solid: A route to fracture?, *Europhys. Lett.*, *46*, 217–223.

Kassner, K., C. Misbah, J. Müller, J. Kappey, and P. Kohlert (2001), Phase-field modeling of stress-induced instabilities, *Phys. Rev. E*, *63*, 036117.

Koehn, D., D. K. Dysthe, and B. Jamtveit (2004), Transient dissolution patterns on stressed crystal surfaces, *Geochim. Cosmochim. Acta*, in press.

Mersmann, A. (1990), Calculation of interfacial tensions, *J. Crystal Growth*, *102*, 841–847.

Parks, G. A. (1984), Surface and interfacial free energies of quartz, *J. Geophys. Res.*, *89*, 3997–4008.

Rimstidt, J. D., and H. L. Barnes (1980), The kinetics of silica water reactions, *Geochim. Cosmochim. Acta*, *44*, 1683–1699.

Ristic, R. I., J. N. Sherwood, and K. Wojciechowski (1993), Morphology and growth kinetics of large sodium chlorate crystals grown in the presence and absence of sodium dithionate impurity, *J. Phys.*, *97*, 10,774–10,782.

Srolovitz, D. J. (1989), Surface morphology evolution in stressed solids: Surface diffusion controlled crack initiation, *Acta Metall.*, *37*, 621–625.

Yang, W. H., and D. J. Srolovitz (1993), Cracklike surface instabilities in stressed solids, *Phys. Rev. Lett.*, *71*, 1593–1596.

J.-P. Gratier and F. Renard, LGIT-CNRS-Observatoire, Université Joseph Fourier, F-38041 Grenoble, France. (francois.renard@obs.ujf-grenoble.fr)

K. Kassner, Institut für Theoretische Physik, Otto-von-Guericke-Universität Magdeburg, Postfach 4120, D-39016 Magdeburg, Germany.

C. Misbah, Groupe de Recherche sur les Phénomènes Hors de l'Equilibre, LSP, Université Joseph Fourier (CNRS), Grenoble I, B.P. 87, F-38402 Saint-Martin d'Hères Cedex, France.